# Mechanical properties of nickel-graphene composites synthesized by electrochemical deposition

Zhaodi Ren[1], Khurram Shehzad[1], Nan Meng[1], Yang Xu[1 a)], Shaoxing Qu[2], Bin Yu[3,1] and J.K. Luo[4,1]

[1]Department of Information Science and Electronic Engineering, Zhejiang University, Hangzhou 310027, China

[2] Department of Engineering Mechanics, Zhejiang University, Hangzhou 310027, China

[3]College of Nanoscale Science and Engineering, State University of New York, Albany, New York 12203, USA

[4]Inst. of Renew. Energ. & Environ. Technol., University of Bolton, Deane Road, Bolton, BL3 5AB, United Kingdom.

[a)] Author to whom correspondence should be addressed.

Electronic addresses: yangxu-isee@zju.edu.cn

**Abstract**: Graphene (Gr) nanoflakes with multi-layer structures were dispersed in the nickel (Ni) plating solution by using surfactant and magnetic stirring method. Gr flakes were co-deposited with the Ni crystalline through plating process to form Ni-Gr composites on a substrate. Gr was uniformly dispersed in the Ni matrix and the oxygen radicals present in the Gr were reduced during the electro-deposition process. Incorporation of Gr in the Ni matrix increased both the inter-planar spacing and the degree of preferred orientation of Ni crystalline. The elastic modulus and hardness of the Ni-Gr composites reached 240 GPa and 4.6 GPa respectively, which are about 1.7 and 1.2 times that of the pure Ni deposited at the same condition. The increase in the mechanical properties of the composites is attributed to preferred formation of the Ni crystalline phases in its (111) plane, high interaction between Ni and Gr, and the excellent intrinsic mechanical properties of Gr. Results suggest that this method of using Gr directly instead of GO is efficient and scalable to be used in industry.

Keywords: nickel-graphene composites, mechanical properties, electrochemical deposition

## Introduction

Two dimensional (2D) materials, especially graphene (Gr), have received great interests since Gr nanoflakes were first obtained by a simple mechanical exfoliation method in 2004[1]. Gr has excellent electrical, thermal, and mechanical properties [2-5]. Mechanical measurements show that perfect single-layer graphene exhibits a Young's modulus (E) of 1.0 TPa and a fracture strength of 130 GPa. Such extraordinary mechanical properties make them potentially valuable materials for their use as a reinforcing medium [6]. Gr has been used to reinforce the polymer and metals to improve their mechanical properties. With the addition of Gr into Al [7,8], Cu[9], and Mg[10] matrices by powder metallurgy routes, into Cu[11] and Ni[12] by direct current (DC) electro deposition, and into Cu[13] by a molecular mixing process, dramatic improvements in mechanical properties of the respective composites have been achieved. Ni-based composites have been widely adopted in automobile and aerospace industries because of their high specific strength, favorable wear and corrosion resistance, and high toughness [14-17]. Ni composites are usually reinforced with fibers or nanoparticles to improve their mechanical properties while keeping their excellent thermal and electrical conductivities. CNT is one of the most widely used materials to strengthen the Ni matrix and the mechanical property of the Ni matrix is improved greatly by the addition of CNT [18]. As another novel member of carbon family, Gr is also been expected to significantly increase the hardness and Young's modulus of the Ni matrix as that of CNT[19-23]. Furthermore, as a 2D material, Gr-Ni composites are expected to have higher force transmission than that of CNT. Ni-Gr composites thus have great interests and have been widely prepared by electro deposition method [21,22]. By using this method, GO was dispersed in the plating solution to form Ni-GO composites firstly owing to its stable dispersion in water since Gr is not dissolved in water, and then GO in the Ni-GO composites is reduced at high temperature to from Ni-Gr composites[21,22]. However, the challenge of the method is the high temperature technology used for reducing GO to Gr, which not only decreases the density of the Ni composites but also complicates the quality control of the Ni crystalline formation. Furthermore, the mechanisms for the formation and the improvement in the mechanical properties of Ni-Gr composites have seldom been studied in detail previously.

In this work, by using a surfactant and applying vigorous stirring conditions, Gr (instead of GO) was dispersed in the Ni plating solution. Ni-Gr composites were electro deposited directly onto a steel substrate without further processing. Both the formation and the mechanical property of the Ni-Gr composites as-prepared have been investigated. The reinforcement mechanism is also discussed in detail.

**Deposition experimental and material characterization**

Ni and Ni-Gr composites were synthesized by electroplating method. Gr nanoflakes of multilayer with thickness of 3-5 nm synthesized by using GO as the source material through high temperature reduction [24] were used in the deposition.

The Ni plating solution consisted of $NiSO_4 \cdot 7H_2O$ (300 g/L), $NiCl_2 \cdot 6H_2O$ (35 g/L), $H_3BO_3$ (40 g/L) and surfactant (0.5g/L). After the Ni plating solution being prepared, Gr nanoflakes of 0.05g/L were added to the Ni plating solution, which was stirred continuously for at least 10 min before deposition and during the whole plating process at a rate of 300 rpm. Steel plates with dimensions of 2 cm × 2 cm, thickness of 1 mm were used as the cathode substrate and Ni plate as the anode. Before plating, steel substrates were washed with a mixed solution of NaOH (30 g/L), $Na_3PO_4$ (30 g/L), $Na_2CO_3$ (30 g/L), and $Na_2SiO_3$ (10 g/L) at 80$^{\circ}$C for 10 min, followed by electrochemical wash and then activation in 30% HCl for 2 min. The plating was performed at 50 $^{\circ}$C with the current density varied from 0.15 to 4 A/dm$^2$ and it was lasted for 1-3 hr. The samples were polished using diamond polishing liquid to obtain a relatively constant thickness of roughly 5~10μm for different current densities before the nano-indentation measurement. Pure Ni was also synthesized under the same condition for comparison with no Gr nanoflakes in the solution. The plating process is schematically illustrated in Fig.1.

Ni and Ni-Gr composite samples were characterized by Raman spectrocopy (inVia-Reflex, Renishaw plc, 514 nm laser), X-ray photoelectron spectroscopy (XPS, VG ESCALAB MARK II® system, VG instruments, Al Ka, 5kV), X-ray diffraction (XRD, Empyrean Panalytical 200895, Cu, Kα), EDS, and scanning electron microscopy (SEM, Hitachi S-4800), Nano indentation (TriboIndenter, load 5s, hold 5s, unload 5s, the maximum force is 5 mN ).

To identify if Gr nanoflakes are incorporated inside the Ni film, the deposited Gr-Ni

composite films were polished using XXX to remove approximately X-X μm of the top layer, then they were characterized by various methods.

## Results and discussion

### Crystal structure characterization

XRD patterns of the Ni-Gr composites synthesized under various plating current densities are shown in Fig. 2a. The results indicate that the cubic structured Ni crystalline phase is formed for the Ni-Gr composites, similar to that of the pure Ni shown in Fig. 2b. XRD peaks corresponding to Gr (around $26^{\circ}$) as shown in Fig. S1b were not observed, most probably because of the much low intensity of the Gr peaks compared to that of the Ni crystalline peaks. However, the Raman spectra clearly show the presence of Gr in the Ni-Gr composites, where the G, D, and 2D bands characteristic of Gr were observed at the wave numbers of 1580, 1350 and 2920 $cm^{-1}$, respectively, as shown in Fig. S2-S3. As shown in Fig. 3a and 3b, the C distribution in Ni-Gr composites is uniform, indicating the uniform distribution of Gr in the Ni matrix. After being polished, the Gr in the Ni matrix is exposed on the surface of the Ni matrix and there are more C and O atoms present in these areas compared to other areas as shown in Fig. 3c-3f. The increase of oxygen content in the areas where Gr existed is probably due to the existence of oxygen radicals that remained in the source Gr nanoflakes being used [24], as exhibited by the XPS analysis of the Gr as shown in Fig. S1a. The grain size synthesized by lower current density is smaller than that by higher current density, which results in a higher density of interfaces for the lower current density sample than that of higher current density sample as shown in Fig. 3g-3l.

The $SP^2$ C-C content in Gr can be obtained from the XPS peak ratios. As shown in Fig. 4, the $SP^2$ C-C content is 71.4% and 83.9% in Gr and Ni-Gr composites respectively, indicating that the oxygen radicals remained in Gr are reduced further when incorporated into the Ni matrix by plating method[25,26]. It was also confirmed by the Raman results, which will be discussed below.

### Mechanical Properties characterization

Fig. 5a and 4b shows the load and unload curves of both Ni-Gr composite and pure Ni, indicating that mechanical properties are improved with the incorporation of Gr. Fig. 5c

illustrates that the elastic modulus (E) and the hardness (H) increase from 137-183 GPa and 3.0-4.1 GPa for the pure Ni to 203-239 GPa and 3.3-4.6 GPa for the Ni-Gr composites, respectively.

The grain size of the Ni-Gr composites is larger than that of the pure Ni and it is increased linearly with the increase of current density compared to that of the pure Ni as shown in Fig. 6a and 6b respectively. The hardness of the Ni-Gr should be decreased with the increase of the plating current density due to the grain coarsening as shown in Fig. 6b. However, as shown in Fig. 6l, the hardness ratio increases with the plating current density. It indicates that there are others factors besides the grain size that may affect the hardness of the Ni-Gr composites. As shown in Fig. 6j and 6l, the elastic modulus varies in the opposite direction with that of the hardness with the increase of current density. As exhibited by the variation of $I_{111}/I_{220}$ in Fig. 6d and elastic modulus in Fig. 6j combined with Gr contents in Fig. 2e at high plating current density, both the orientation degree of the Ni crystalline and the Gr contents have an effect on the elastic modulus and hardness of the Ni-Gr composites. It shows that the variation of elastic modulus in the Ni-Gr composites is mainly depends on the orientation growth of Ni(111) plane and the Gr contents. As shown in the Fig. 6c and 6d, with the incorporation of Gr in the Ni matrix, the relative intensity of Ni (111) increases in the Ni-Gr composites compared with that of the pure Ni, which shows that Gr is energy favorable for formation of Ni crystalline in Ni (111) and Ni(220), thus preventing its growth in Ni(200) direction. The higher elastic modulus is easily to be obtained at higher orientation degree of Ni(111) as well as the higher Gr contents as exhibited by the combination of Fig.6c,d,i,j and Fig.2e. The elastic modulus of Ni(111) is higher than that of other planes and thus the increase in the orientation growth in Ni(111) can increase the elastic modulus of the Ni-Gr composites[27]. The effect of Gr on the elastic modulus of the Ni-Gr involves several aspects. Firstly, the elastic modulus of Gr is higher than that of Ni matrix and thus the higher Gr contents results in the higher elastic modulus of the Ni-Gr composites. Secondly, Gr can prevent the slide of the dislocation in the Ni matrix and thus will induce the increase of the elastic modulus in the Ni-Gr composites. However, the variation of hardness is different than that of elastic modulus with the increase of plating current density as shown in Fig. 6i-6l. It is probably due to the reason as follows. Firstly, the variation in the interface quantities between

different planes that induced by the variation of the orientation growth of Ni(111) plane will induce the hardness variation in the opposite direction compared to that of elastic modulus. Secondly, the decrease of hardness at high plating current density is probably due to the grain coarsening while the decrease of hardness at low plating current density is probably due to the increase of the slide between layers of Gr. Almost at all current densities, Ni grain size in the Ni-Gr composites is relatively larger and experiences steeper increase with current density than that of the pure Ni, which might be due to the increase in the growth rate of Ni (111) plane and can also be confirmed from SEM shown in Fig. 3g-3l. The larger grain size and the higher orientation of the Ni crystalline phase can benefit the improvement of the elastic modulus while can decrease the hardness of the Ni-Gr composites due to the lower quantity of boundary interfaces with lower elastic modulus and the higher elastic modulus of (111) plane than others plane.

Fig. 6e-6h show the variation of $D_{FWHM,}$ 2D peak shift, $I_D/I_G$, and $I_{2D}/I_G$ of Gr in the Ni-Gr composites compared with that of the original Gr. With increase of Gr content, the relative thinner Ni metal plays less effect on Gr and results in the lower $D_{FWHM}$. XPS was used to further confirm the reduction of Gr and to calculate the degree of reduction during the electro deposition process as discussed above. The further reduction of oxygen radicals in the Gr decreases the adverse effect of the oxygen radicals on the mechanical property of the Gr and results in the better mechanical property of Ni-Gr composites.

Another reason for the improved mechanical properties of the Ni-Gr composites is that Ni and Gr has relatively strong interaction, indicated by their strong interaction energy (24 ev)[20] and the high solubility of the C in the Ni[28]. Moreover, the –COOH and –OH groups attached to the Gr (EDS results in Fig. 3 prove the existence of oxygen related groups in Gr) are expected to form covalent bonds between Ni and the Gr. These types of covalent bond between metal and Gr, and between metal and CNTs have been reported previously [13,29]. Inter-planar spacing parameter, $d_{Ni}$ (111), presented in Fig. 2d clearly shows that the Gr has been incorporated between the planes, due to its strong interaction with Ni, and has distorted the Ni crystalline structure. No formation of second phase shows that C is dissolved in Ni lattice and stress is produced for Ni matrix to sustain the lattice location. As shown in Fig. 2d, this distortion or inter-planar spacing value is larger for the lower plating current density. Both

of these factors, Ni-Gr interaction and the covalent bonds between Ni and Gr, result in the Ni-Gr interfaces that can transfer the load more effectively which lead to the improved mechanical properties. Previous study on metal-graphene layered structures have reported that the presence of even a single atomic layer of graphene between the metal layers, due to its great mechanical strength and resistance to rupture and shearing can effectively block the propagation of gliding dislocations across the metal-graphene interfaces[20]. We believe that in our Ni-Gr composites, effective load transfer between Ni and Gr due to their strong interaction and the effectiveness of Gr to act as a barrier to dislocation propagation at the higher compressive strains lead to improved values of elastic modulus and hardness compared to the pure Ni.

In summary, The Yong's modulus of the Ni-Gr composites is increased mainly due to the combined effects of high elastic modulus Gr incorporated in the Ni grain, Ni-Gr interaction and the increase in the number of certain Ni crystalline planes with higher elastic modulus values.

## Conclusions

Ni-Gr composites were successful synthesized by electroplating method through adding the Gr nanoflakes directly in the Ni plating solution. Gr nanoflakes were uniformly dispersed in the Ni matrix on its grain surfaces and the grain boundaries. Gr induced morphological changes in the Ni structures, and resulted in Ni-Gr composites with elastic modulus values as large as 240 GPa and hardness as large as 4.6 GPa with additions of Gr only as low as 0.05 $g/L^3$. Reasons for such improved mechanical properties include, excellent intrinsic graphene mechanical properties, Gr induced selective growth of certain crystalline phases of Ni, interaction between Ni matrix and Gr flakes, the prevention of the dislocation glide at the interface of grains by the Gr nanoflakes.

## Acknowledgements

This work was supported by U.S. National Science Foundation (Grants ECCS-1002228, ECCS-1028267, CMMI-1162312), NSFC (Nos. 61274037, 61274123, CPSF2013M541776,

and 61474099) and the Zhejiang Provincial NSF (Nos. LR12F04001 and BSH1301017). The authors also would like to acknowledge the financial support by the Innovation Platform of Micro/Nano devices and Integration System. TH wishes to acknowledge funding from the Royal Academy of Engineering (Graphlex).

**References**


1. K. S. Novoselov, A. K. Geim, S. V. Morozov, D. Jiang, Y. Zhang, S. V. Dubonos, I. V. Grigorieva, A. A. Firsov. Electric Field Effect in Atomically Thin Carbon Films. *Science* **306**, 666(2004).
2. F Scarpa, S Adhikari and A Srikantha Phani. Effective elastic mechanical properties of single layer graphene sheets. *Nanotechnology* **20**,065709(2009).
3. I.A.Ovid'ko. Mechanical property of graphene. *Rev.Adv.Mater.Sci*. **34**,1-11(2013).
4. Ricardo Faccio, Luciana Fernández-Werner, Helena Pardo, Cecilia Goyenola, Pablo A. Denis and Álvaro W.Mombrú. Mechanical and Electronic Properties of Graphene Nanostructures, Physics and Applications of Graphene - Theory, Dr. Sergey Mikhailov (Ed.), ISBN: 978-953-307-152-7, InTech, Available from:http://www.intechopen.com/books/physics-and-applications-of-graphene-theory/mechanical-and-electronicproperties-of-graphene-nanostructures (2011).
5. Ali R. Ranjbartoreh, Bei Wang, Xiaoping Shen, and Guoxiu Wang. Advanced mechanical properties of graphene paper. *Journal of Applied Physics* **109**, 014306 (2011).
6. Sasha Stankovich, Dmitriy A. Dikin, Geoffrey H. B. Dommett, Kevin M. Kohlhaas, Eric J. Zimney,Eric A. Stach, Richard D. Piner, SonBinh T. Nguyen & Rodney S. Ruoff. Graphene-based composite materials. *Nature* **442**, 282-286(2006).
7. Wang, J., et al., Reinforcement with graphene nanosheets in aluminum matrix composites. *Scripta Materialia* **66**(8),594-597(2012).
8. Bartolucci, S.F., et al., Graphene–aluminum nanocomposites. *Materials Science and Engineering: A* **528**(27),7933-7937(2011).
9. Koltsova, T.S., et al., New hybrid copper composite materials based on carbon nanostructures. *Journal of Materials Science and Engineering B* **2**(4), 240-246 (2012).
10. Chen, L.-Y., et al., Novel nanoprocessing route for bulk graphene nanoplatelets reinforced metal matrix nanocomposites. *Scripta Materialia* **67**(1),29-32(2012).
11. Kasichainula Jagannadham. Electrical conductivity of copper–graphene composite films synthesized by electrochemical deposition with exfoliated

graphene platelets. *J. Vac. Sci. Technol. B* **30**(3), 03D109-1(2012).

12. Kuang, D., et al., Graphene–nickel composites. *Applied Surface Science* **273**(0), 484-490 (2013).
13. Hwang,J. et al., Enhanced Mechanical Properties of Graphene/Copper Nanocomposites Using a Molecular-Level Mixing Process. *Advanced Materials* **25**(46), 6724-6729 (2013).
14. Zhou, S., et al., Analysis of crack behavior for Ni-based WC composite coatings by laser cladding and crack-free realization. *Applied Surface Science* **255** (5), 1646-1653 (2008).
15. Lajevardi, S. and T. Shahrabi, Effects of pulse electrodeposition parameters on the properties of Ni–$TiO_2$ nanocomposite coatings. *Applied Surface Science*. **256** (22), 6775-6781(2010).
16. Xu, J., et al., Investigation on corrosion and wear behaviors of nanoparticles reinforced Ni-based composite alloying layer. *Applied Surface Science* **254**(13), 4036-4043 (2008).
17. Zhou, S., et al., Analysis of crack behavior for Ni-based WC composite coatings by laser cladding and crack-free realization. *Applied Surface Science* **255** (5), 1646-1653 (2008).
18. W.X. Chen , J.P. Tu, H.Y. Gan, Z.D. Xu, Q.G. Wang, J.Y. Lee, Z.L. Liu, X.B. Zhang. Electroless preparation and tribological properties of Ni-P-Carbon nanotube composite coatings under lubricated condition. *Surface and Coatings Technology* **160** ,68–73 (2002); Jonathan Nguyen,Troy B. Holland,Haiming Wen,Martin Fraga, Amiya Mukherjee and Enrique Lavernia. Mechanical behavior of ultrafine-grained Ni-carbon nanotube composite. J Mater Sci **49**, 2070–2077(2014).
19. N. K. Mahale, R. D. Ladhe, S. B. Attarde, and S. T. Ingle. Synthesis and the Structural Transformation of fcc to hcp in Ni-Graphene Nanocomposite by Simple Chemical Route via Sonication. *Journal of Nanoparticles* 305637(2014).
20. Youbin Kim, Jinsup Lee, Min Sun Yeom, Jae Won Shin, Hyungjun Kim, Yi Cui, Jeffrey W. Kysar,James Hone, Yousung Jung, Seokwoo Jeon & Seung Min Han. Strengthening effect of single-atomic-layer graphene in metal–graphene

nanolayered composites. *Nature communications* **4** (2113),1-7(2013).

21. Da Kuang, Liye Xu, Lei Liu, Wenbin Hu, Yating Wu. Graphene–nickel composites. *Applied Surface Science* **273**,484–490(2013).
22. Hu Qing-hua, Wang Xi-tang, Chen Hao, Wang Zhou-fu. Synthesis of Ni/Graphene Sheets by an Electroless Ni-Plating Method. *New Carbon Mater.* **27**(1): 35-41 (2012).
23. Preparation and Corrosion Behavior of Ni and Ni–Graphene Composite Coatings. *Mater. Res. Bull.* **48**, 1477–1483(2013).
24. Stankovich, S., et al., Synthesis of graphene-based nanosheets via chemical reduction of exfoliated graphite oxide. *Carbon* **45**(7),1558-1565(2007).
25. Zhou, M., et al., Controlled synthesis of large-area and patterned electrochemically reduced graphene oxide films. *Chemistry - A European Journal* **15** (25), 6116-6120 (2009).
26. An, S.J., et al., Thin film fabrication and simultaneous anodic reduction of deposited graphene oxide platelets by electrophoretic deposition. *The Journal of Physical Chemistry Letters* **1**(8),1259-1263(2010).
27. A. Ibáñez, R. Escudero-Cid, P. Ocón, E. Fatás. Effect of the pulse plating parameters on the mechanical properties of nickel electrodeposits. *Surface & Coatings Technology* **212**, 94–100(2012).
28. Lander, J.J., H.E. Kern, and A.L. Beach, Solubility and Diffusion Coefficient of Carbon in Nickel: Reaction Rates of Nickel-Carbon Alloys with Barium Oxide. *Journal of Applied Physics* **23**(12), 305-1309(1952).
29. Kim, K.T., et al.The Role of Interfacial Oxygen Atoms in the Enhanced Mechanical Properties of Carbon-Nanotube-Reinforced Metal Matrix Nanocomposites. *Small* 4(11), 1936-1940(2008).

# Figures

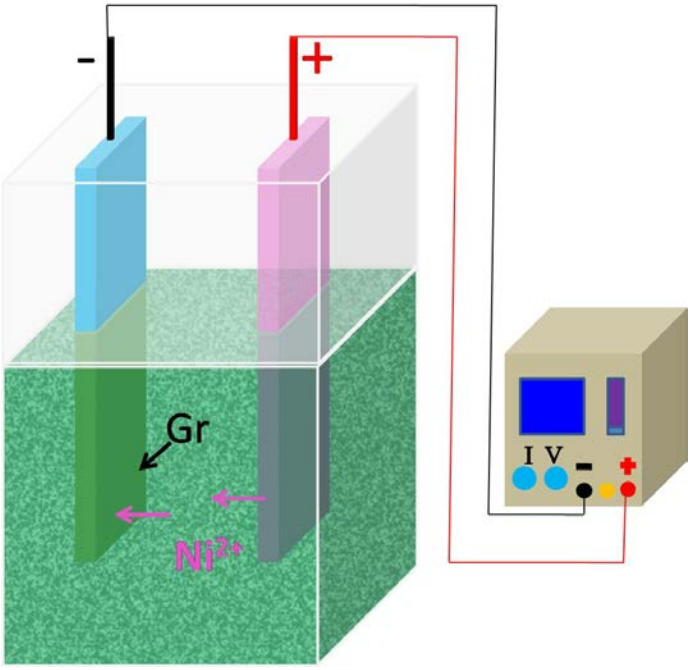


Figure 1. Schematic of the plating process

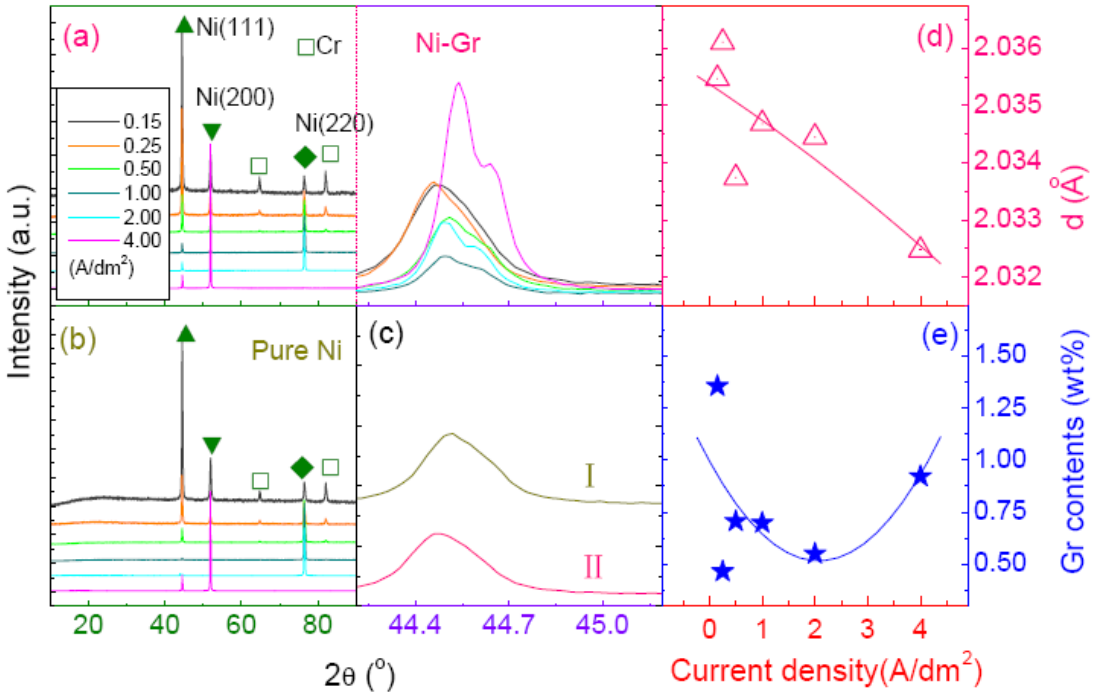


Figure 2. XRD patterns of (a) Ni-Gr, (b) Pure Ni. (c) the Ni(111) peak of (I) pure Ni and (II) Ni-Gr. (d) show the corresponding $d_{Ni(111)}$ in the right of (a), respectively. (e) Gr contents vary with plating current density.

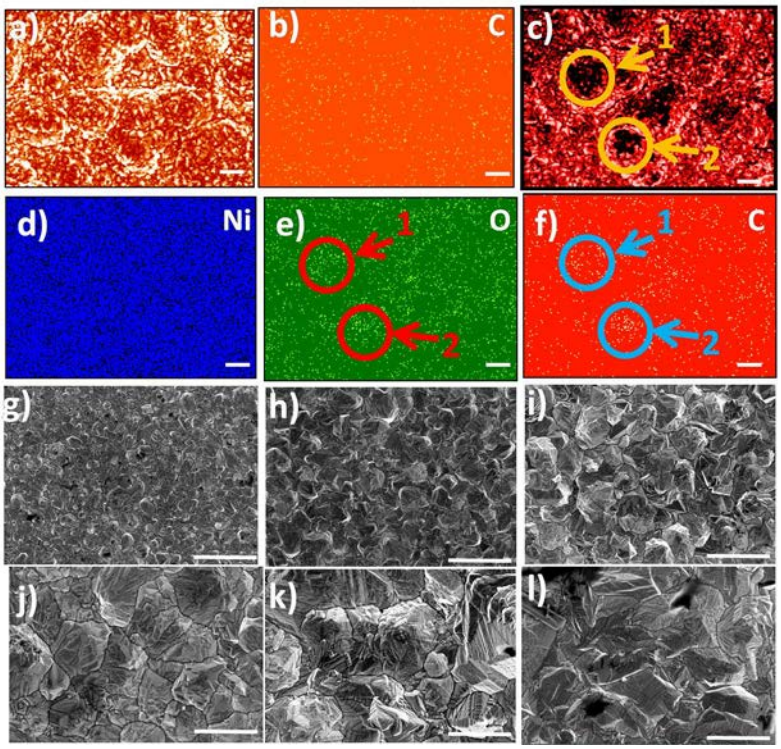


Figure 3. SEM and EDS mapping of Ni-Gr composites. (a) SEM image indicates the distribution of graphene in Ni-Gr composites is uniform. (b) EDS map image of carbon element distribution in (a). (c) Gr is exposed after the sample (a) was polished as exhibited in location 1 and 2. (d-f) is the corresponding EDS map images of Ni, C, and O results, respectively. There are more C and O in the enclosed area at locations of 1 and 2 shown in (b) than other areas, which mean that the incorporated Gr in Ni-Gr composites is exposed after polishing. (g-l) are the Ni-multilayer Gr with plating current densities from 0.15 to 4.00 $A/dm^2$. The scare bars in (a-f) and (g-l) are 5 μm and 3 μm, respectively.

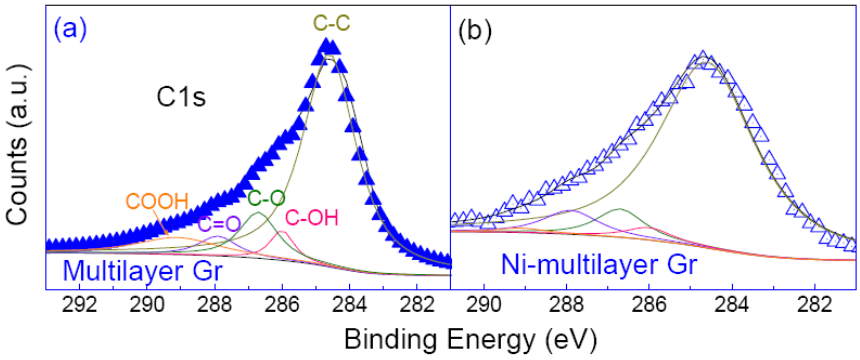


Figure 4. XPS C1s of Gr and Ni-Gr composites with plating current density at 4.00 A/dm$^2$ .

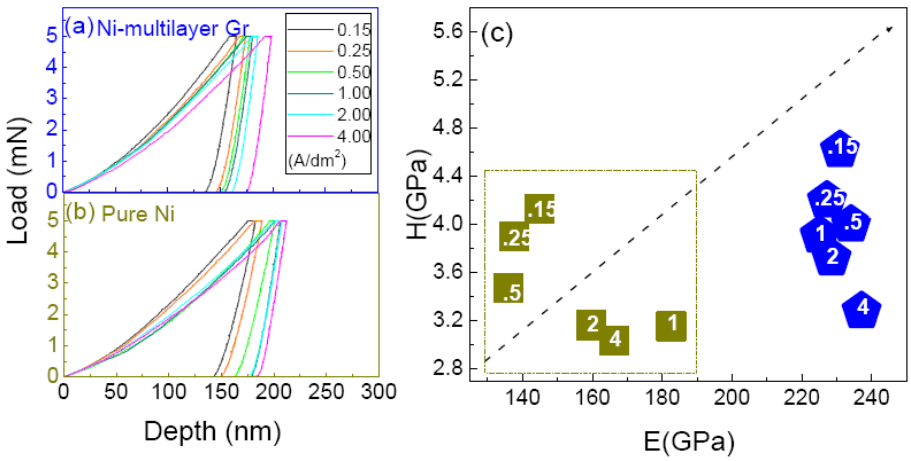


Figure 5. Load-unload curves of (a) Ni-multilayer Gr and (b) Pure Ni with plating current density from 0.15 to 4 A/dm$^2$. (c) the E-H curve of Ni-multilayer Gr (blue), and pure Ni (dark yellow) derived from (a-b). The numbers in (e) denote the plating current density (in A/dm$^2$) .The direction of dashed black arrow indicates the improvement trend for an ideal composite material.

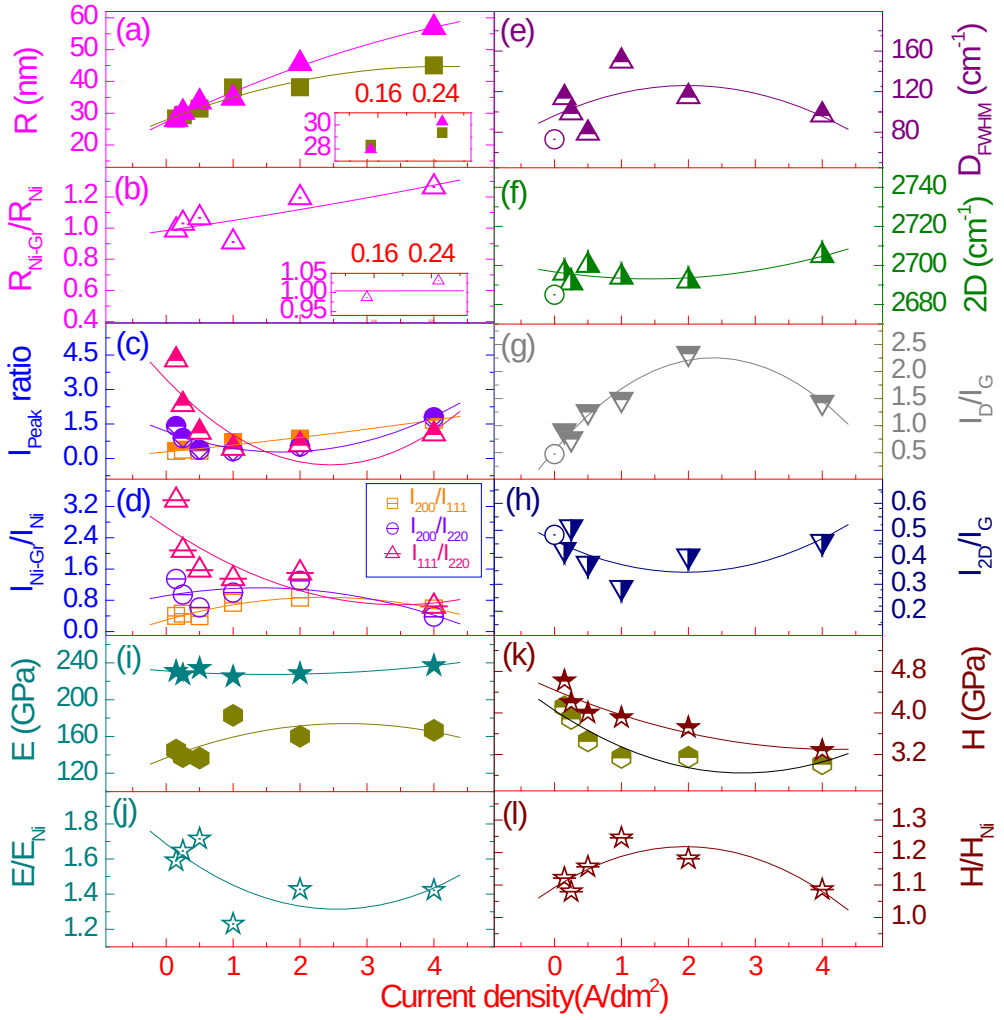


Figure 6. Grain size (a-b), peak intensity ratios from XRD (c-d), Raman parameters (e-h) , E( i, j) and H(k,l) in the Ni-Gr composites vary with plating current density. The data points of pure Ni and Ni-Gr are presented in dark yellow and colorful, respectively. As a reference, the Raman data of as received graphene (colorful) are marked in unfilled circle, respectively. The color in (c) is in accordance with that of in (d).

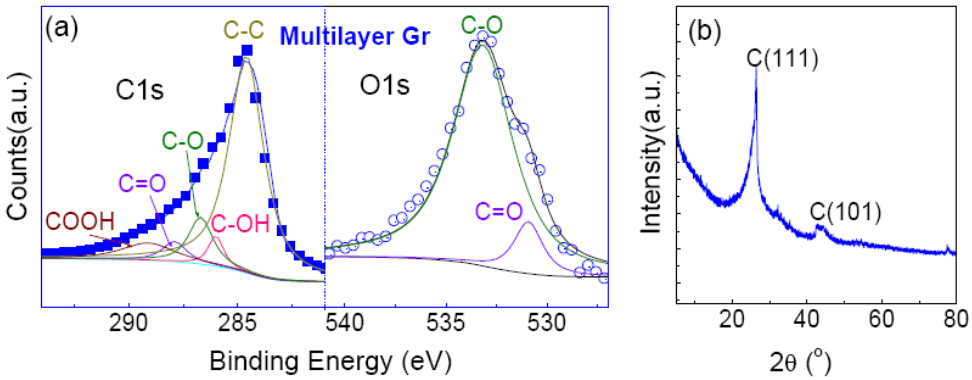


Figure S1. XPS Characterization of graphene used. (a) C 1s and O1s of multilayer Gr and (b) XRD of multilayer Gr (blue).

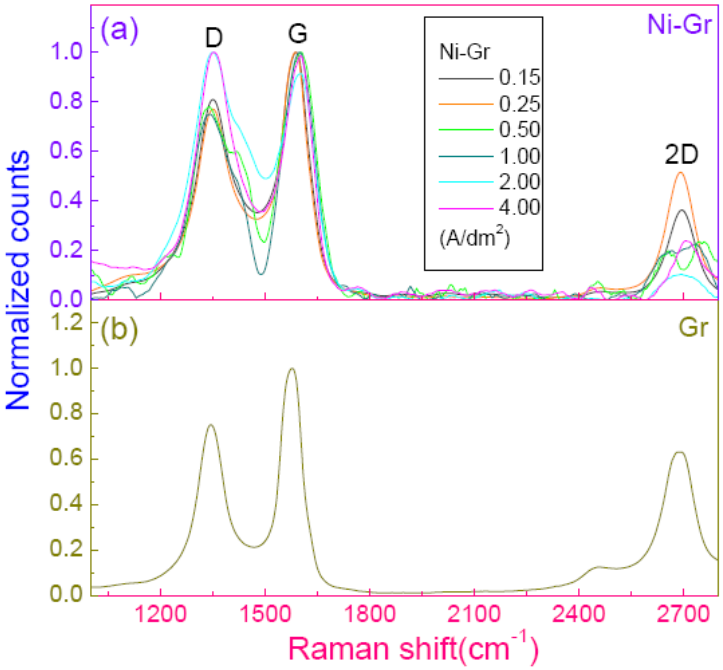


Figure S2. Raman of Gr and Ni-multilayer Gr.

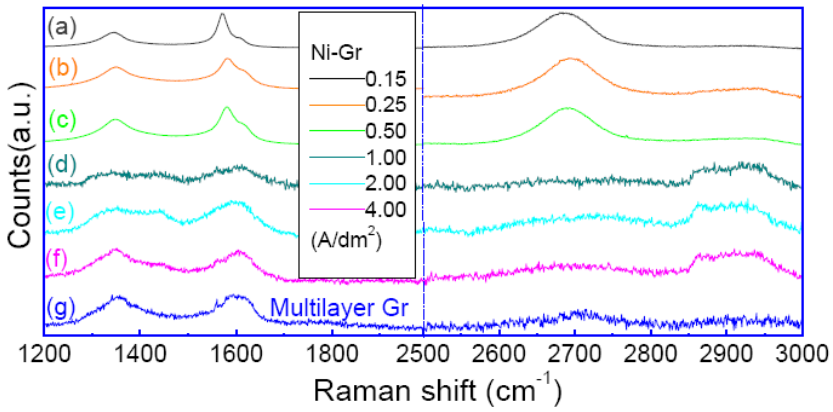


Figure S3. Raman of (a-f) Ni-multilayer Gr composites prepared with current density from 0.15 to 4.00 A/dm$^2$ and (g) multilayer Gr.

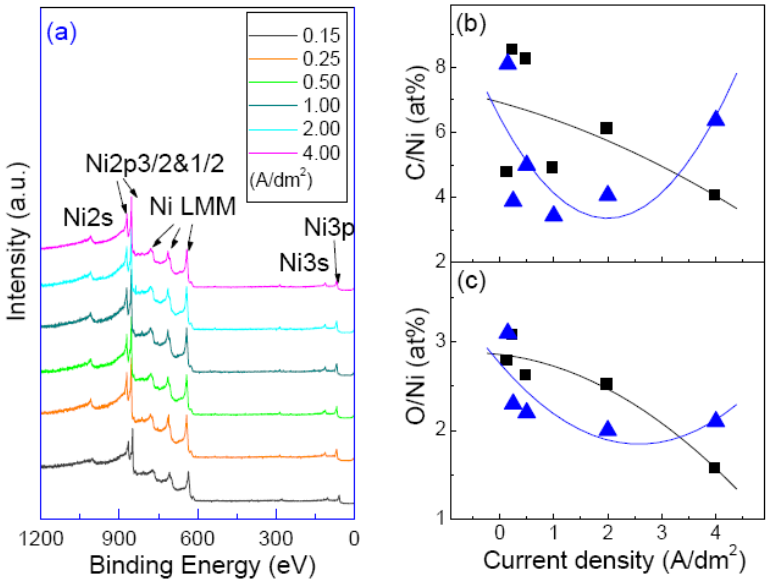


Figure S4. (a) XPS of Ni-multilayer Gr. (b-c) EDS of C/Ni and O/Ni of pure Ni (black), and Ni-multilayer Gr (blue).

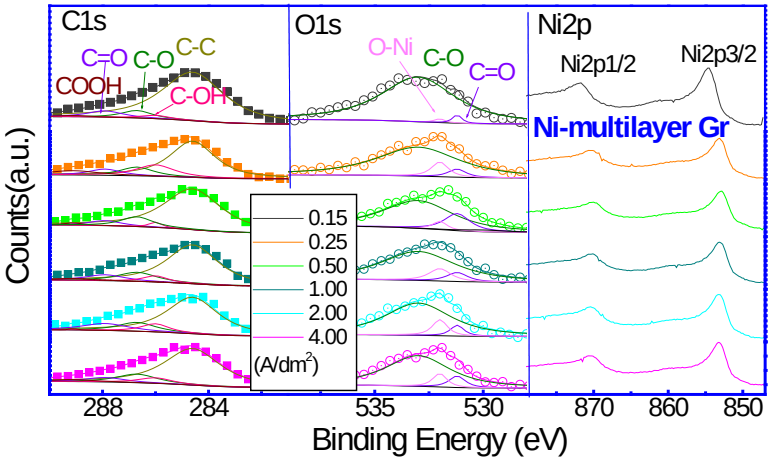


Figure S5. C1S, O1S, and Ni2p of Ni-multilayer Gr (blue).

Table S1. Relative contents of C radicals from C1s,O1s, and Ni2p peaks of XPS

| | | C1s | | | | | |
|---|---|---|---|---|---|---|---|
| | | C-C | C-O | C=O | COOH | C-OH | Total area |
| Multilayer Gr | | 71.3 | 10.8 | 4.7 | 8.8 | 4.4 | 7034 |
| Ni-multilayer Gr ($A/dm^2$) | 0.15 | 83.9 | 6.3 | 6.1 | 1.0 | 2.7 | 2071 |
| | 0.25 | 59.0 | 10.5 | 7.2 | 7.8 | 15.5 | 1302 |
| | 0.5 | 80.1 | 10.6 | 5.6 | 1.5 | 2.2 | 1647 |
| | 1 | 71.5 | 12.6 | 8.2 | 2.2 | 5.5 | 1222 |
| | 2 | 68.0 | 12.0 | 11.6 | 0.4 | 8.1 | 1387 |
| | 4 | 72.1 | 12.1 | 6.2 | 3.0 | 6.5 | 1956 |
| | | O1s | | | | $Ni_{2p3/2}$ | |
| | | C-O | C=O | O-Ni | Total area | Total area | |
| Multilayer Gr | | 89.9 | 10.1 | - | 1909 | - | |
| Ni-multilayer Gr ($A/dm^2$) | 0.15 | 96.7 | 2.2 | 1.1 | 883 | 25563 | |
| | 0.25 | 86.0 | 5.1 | 8.8 | 816 | 33521 | |
| | 0.5 | 75.4 | 16.9 | 7.7 | 798 | 33033 | |
| | 1 | 82.6 | 7.1 | 10.3 | 691 | 35586 | |
| | 2 | 84.7 | 5.8 | 9.5 | 737 | 34181 | |
| | 4 | 83.9 | 8.0 | 8.1 | 688 | 30689 | |